References

[1] Likins, P. W., and Gale, A. H., "The Analysis of Interactions Between Attitude Control Systems and Flexible Appendages," IAF AD29, 19th International Astronautical Congress, New York, Oct. 13–18, 1968.

[2] Yu, Y. Y., "Stability of Nonlinear Attitude Control System Including Particularly Effect of Large Deflection of Space Vehicles," IAF AT35, 19th International Astronautical Congress, New York, Oct. 13–18, 1968.

[3] Gevarter, W. B., "Basic Relations for Control of Flexible Vehicles," *AIAA Journal*, Vol. 8, No. 4, April 1970, pp. 666–672.

[4] Noll, R. B., Deyst, J. J., Jr., and Spenny, C. H., "A Survey of Structural Flexibility Effects on Spacecraft Control Systems," AIAA Paper 69-116, New York, 1969.

[5] *Effects of Structural Flexibility on Spacecraft Control Systems*, NASA Space Vehicle Design Criteria Document, NASA SP-8016, April 1969.

[6] Hooker, W. W., and Margulies, G., "The Dynamical Attitude Equations for an N-Body Satellite," *Journal of the Astronautical Sciences*, Vol. 12, No. 4, 1965, pp. 123–128.

[7] Roberson, R. E. and Wittenburg, J., "A Dynamical Formalism for an Arbitrary Number of Interconnected Rigid Bodies, with Reference to the Problem of Satellite Attitude Control," *Proceedings of the 3rd International Congress of Automatic Control*, Butterworth, London, 1967.

[8] Fleischer, G. E., "Multi-Rigid-Body Attitude Dynamics Simulation," TR 32-1516, Feb. 15, 1971, Jet Propulsion Lab., Pasadena, Calif.

[9] Russell, W. J., "On the Formulation of Euations of Rotational Motion for an N-Body Spacecraft," Rept. TR-0200(4133)-2, 1969, Aerospace Corp., El Segundo, Calif.

[10] Likins, P. W., "Dynamics and Control of Flexible Space Vehicles," TR 32-1329, Rev. 1, 1970, Jet Propulsion Lab., Pasadena, Calif.

[11] Gale, A. H. and Likins, P. W., "Influence of Flexible Appendages on Dual-Spin Spacecraft Dynamics and Control," *Journal of Spacecraft and Rockets*, Vol. 7, No. 9, Sept. 1970, pp. 1049–1056.

[12] Kopf, E. H., "A Mariner Orbiter Autopilot Design," TR 32-1349, 1969, Jet Propulsion Lab., Pasadena, Calif.

MARCH 1971 J. SPACECRAFT VOL. 8, NO. 3

Development of a Biowaste Resistojet

CARL R. HALBACH* AND RONALD Y. YOSHIDA†
The Marquardt Company, Van Nuys, Calif.

The 10-mlb-thrust, concentric-tubes resistojet is being developed for use with biowaste propellants. The selection of a suitable material for the thruster heater parts is discussed; platinum-20% iridium is the present choice. Emphasis is placed on the problems of carbon deposition with propellant mixtures containing methane and of carbonyl attack by CO_2. The biowaste resistojets have been strengthened to withstand launch vibration and acceleration loads, and the Mark II model has a trumpet-shaped nozzle with an expansion ratio of 400. Thrusting performance for methane, carbon dioxide, water, hydrogen, and typical biowaste propellant mixtures is presented.

Introduction

STUDIES of manned space stations show that some waste products (e. g., CH_4, CO_2, H_2O, and H_2) from the life support systems will be available for use as rocket propellants for attitude-control and station-keeping propulsion. The biowaste propulsion system becomes part of a mass-conservative attitude-control system utilizing control moment gyros.[1] This paper presents a status report on a program[2] to develop 10-mlb-thrust resistojets for this purpose, using the life-test-proven[3] concentric-tubes resistojet concept shown schematically in Fig. 1. It consists basically of an electric-resistance-heated, 3-pass heat exchanger and a nozzle for accelerating the heated gas. The electrical flow is through the outer case, nozzle, and inner heating elements; 85% of the ohmic heating takes place in the inner heating element. This design offers the following advantages relative to a single-tube-type resistojet: high thermal efficiency for low power consumption, final gas temperature close to maximum wall temperature for high specific impulse, minimized creep stresses with zero hoop-creep stress in the hottest inner element for long life, and a higher-voltage, lower-current power characteristic, which is desirable. The biopropellants can include mixtures which range through oxidizing, reducing and carburizing atmospheres. Thruster design changes relative to the life-tested thruster include heater material and adaptation of the structure for launch vibration-acceleration load handling capability.

Recieved August 18, 1970; presented as Paper 70-1133 at the AIAA 8th Electric Propulsion Conference, Stanford, Calif., August 31–September 2,1970; revision received November 16, 1970. Work supported by NASA Langley Contract NAS1-9474.

* Senior Project Engineer, Propulsion Division. Member AIAA.

† Program Manager, Propulsion Division. Member AIAA.

Heater Material Selection

The concentric-tubes resistojet in the thin-walled, high-efficiency configuration requires the use of ductile metal heater elements. The structural geometry in this design concept is not compatible with the brittleness and poor shock

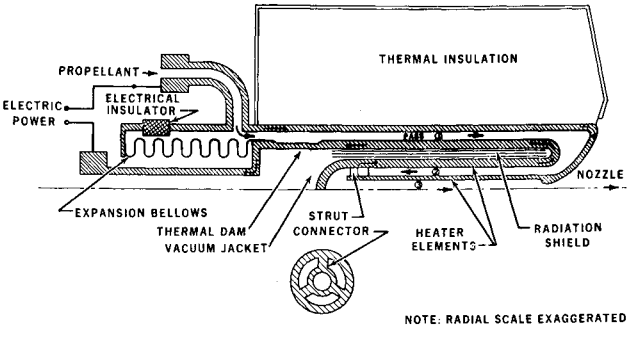

Fig. 1 Evacuated concentric-tubes resistojet concept.

resistance of ceramic materials. Whereas metal coatings are possible, inspection of assembled heaters is difficult, and the reliability for lifetimes of thousands of hours would be low. Metals which protect themselves against oxidation by generating oxide coatings must be avoided, because the oxide film will flake under cyclic thermal mechanical stresses and will be incompatible with the atmospheres whose chemistry is cycling (oxidizing to reducing to carburizing, etc.). A heater material selection study for a high-temperature biowaste resistojet logically suggests the noble metals. A definite selection is difficult because of the lack of corrosion data for candidate materials with the various biopropellant chemistries.

Corrosion resistance is a primary selection criterion. Other considerations include sufficient creep strength at high temperature to withstand thermal-mechanical stresses, sufficient cold mechanical strength to withstand the launch vibration and acceleration loads, and fabricability. An electrical resistivity which is high and which increases with temperature is desirable. A low emissivity is desirable to reduce radial heat transfer by radiation.

Maximum heater temperatures are most likely dictated by required corrosion resistance and creep strength. Creep stress in the inner heater element due to thermal expansion is kept below 50 psi by an expansion bellows. Vibration-acceleration induced stresses are most severe in the innermost heater element when inertia forces are along the thrust axis. An adequate modulus of elasticity and yield strength are required for these stresses. Assuming acceptance testing will be required before launch, yield strength must be sufficient in the annealed condition. Ease of fabrication is desirable. However, experience with the life-tested rhenium resistojet and with the biowaste resistojet suggests fabricability is a "take what you get" factor. If a material of suitable strength and corrosion resistance can be found, ways to form and join it will be found.

Electrical resistivity and its temperature-dependence are important. For a given ohmic-heating distribution, the innermost heater tube can be relatively thicker if its resistivity increases with temperature. A material with a higher resistivity will permit thicker tubes for the same voltage-current characteristic. Thus, greater corrosion rates would be allowed for materials with higher resistance or with positive temperature sensitivity. Differences in electrical resistivity need, therefore, to be normalized in terms of geometry if fair comparisons are to be made.

Although many candidate materials have been considered, development efforts have concentrated on the noble metals. The first three biowaste resistojets fabricated had heater and nozzle parts made of platinum-20% rhodium alloy. This alloy has sufficient mechanical strength and excellent oxidation resistance, but suffers severe corrosion in the presence of CO_2.

A bell-jar experiment has been used to evaluate sample heater tubes. Three samples are tested simultaneously. The tubes are heated electrically and are exposed to vacuum on the outside. Typical propellants at 2 to 3 atm pressure are passed through the tubes. Proper chemistry, temperature, and flow rate are simulated to evaluate corrosion mechanisms while exposing the tube to a hydrostatic bursting creep stress. In effect, these tests simulate the combined environments of the innermost and outer heater tubes of the resistojet simultaneously. Tube samples tested are typically 0.040-in.-i.d. by 0.007-in. wall thickness, simulating the innermost element geometry. Pt-20Rh tube samples were found to fail due to leakage after 500 to 600 hr exposure to CO_2 with wall temperatures from 2700 to 2900°R. Rhodium carbonyls formed and depleted the rhodium from the alloy leaving large voids in the tube walls. Thoria dispersion strengthened platinum was also considered. Although this material did not suffer from carbonyl corrosion, it was found to lack both sufficient mechanical strength and suitable quality for the present generation of resistojet thrusters. Dispersion-strengthened platinum alloys should be developed further for the next generation. Alloys are recommended to achieve high yield strength and modulus with small additions of dispersant to achieve greater creep strength.

Platinum-iridium alloy has been chosen for heater-nozzle parts in the biowaste resistojet. Relative to Pt-Rh, this alloy offers higher mechanical strength and higher resistivity; however, it is more difficult to form and machine. Oxidation resistance is reduced with the addition of iridium in platinum. Relative to pure platinum and Pt-Rh alloys, oxidation rates in air increase an order of magnitude for 10% Ir in platinum. Fortunately, biowaste mixtures do not contain appreciable amounts of oxygen. Decomposition of oxygen-bearing compounds is only partially complete with the relatively short stay times in the resistojet.

Carbonyl corrosion of Pt-30 Ir has been evaluated in the bell jar. A tube sample was exposed to CO_2 for 706 hr with a wall temperature of 2800°R. Post-test examination revealed that there was neither significant carbonyl corrosion nor loss of material by oxidation.

Propellant Chemistry Considerations

The biowaste resistojet was operated with mixtures of CO_2 and methane. Run times were several hours. For an equimolar mixture and mixtures lean in methane, thrust remained constant. Thrust decreased slowly with methane-rich mixtures, more rapidly as the amount of methane increased. The thrust reduction was attributed to nozzle throat size reduction as the result of carbon deposition. The rates of thrust decrease were 0, 0.25, 1.1 and 18.5%/hr for CO_2/CH_4 weight ratios of 2.75 (equimolar), 2.50, 2.0, and 0 (pure methane), respectively. An obvious conclusion is that the more methane in the mixture the more rapid is carbon deposition. However, tests with sample heater tubes in the bell jar indicate that carbon deposition phenomena are quite complex and inconsistent.

Propellant stay times in the thruster are very short: 30, 2, and 0.5 msec in passes 1, 2 and 3, respectively (see Fig. 1). Temperatures are not significant until pass 2 is reached; thus, an effective stay time from a kinetics point of view is of the order of 2 msec. Tables 1 and 2 present kinetic solution data for methane and for the equimolar CO_2-CH_4 mixture. These solutions are for a gas at relatively high temperature (2600°R) in a noncatalytic environment. These data show that the amount of solid carbon formed by thermal decomposition at 2600°R in a few msec is essentially insignificant with mole fractions of the order of 10^{-6}. 2600°R is representative of the effective gas temperature in the thruster. Thermal decomposition of methane can become significant at temperatures above 3000°R. Carbon formed in the bulk gas can subsequently deposit on thruster heater surfaces leaving an amorphous carbon coating. Of greater significance, however, is the formation of pyrolytic carbon on the heater walls. Pyrolytic carbon deposits are the result of an ordered deposit of carbon molecules and occur when carbon bearing molecules are adsorbed on a surface and subsequently decomposed leaving carbon molecules behind.

Intermediate reactions and their kinetics can be significant and must be considered. Heater surface reactions are dependent on local molecular velocities which provide a steady supply of reactants. Gas-stream-directed velocity is much smaller than the molecular velocities. The directed velocity does determine the stay time important in defining the degree of reactions occurring in the bulk of the gas stream. The directed velocity can affect gas-to-wall reactions if diffusion processes are controlling; however, these are considered to be of second order. Directed velocity can have an influence

Table 1 Degree of methane dissociation to solid carbon at 2600°R and 2 atm

Elapsed time, msec	Mixture molecular weight	Mole fractions CH_4	Mole fractions H_2	Solid carbon
1.262	15.48	0.9064	0.0657	0.79×10^{-6}
4.596	15.01	0.8423	0.1159	0.76×10^{-5}
12.05	14.70	0.7848	0.1600	0.326×10^{-4}

through surface erosion and by transporting reaction products to downstream locations.

Catalytic activity of heater surfaces affects initial surface reaction rates. Pyrolytic carbon deposition by decomposition of adsorbed methane molecules, for example, should proceed at a more rapid rate with a material having a high catalytic activity. However, once a molecular layer of carbon is laid down, carbon deposition should proceed at the same rate for all heater materials, regardless of catalytic activity. Here, the decomposition is considered to be the result of gas looking at a carbon surface.

Carbon deposition should be avoided, because long-term accumulation would present a failure mode. Moreover, thrust would be affected by nozzle throat deposits, unless supply pressure were adjusted, and carbon deposits would increase heater surface emissivity, shifting thermal performance to lower efficiency. Carbon deposits can be removed by operating the resistojet with oxygen-bearing gases. This introduces an operational complexity which should be avoided.

Bell-jar tests of heater-tube samples are being conducted to evaluate carbon formation in terms of propellant mixture composition and tube-wall temperature T_w. Sufficient data have been obtained with a CO_2/CH_4 weight ratio of unity to establish a carbon-formation threshold temperature. Figure 2 shows average pyrolytic carbon deposition rate vs T_w. Both Hastelloy X and platinum-20 rhodium tubes were used. Three data points establish the threshold T_w to be 1960°R for the particular mixture. Deposition rate increases rapidly with T_w above the threshold value. The thickest carbon deposit observed was 0.007-in. for the highest temperature Pt-20Rh point. The curve fit is conservative to indicate a maximum expected deposition rate. Although not conclusive, the Pt-20Rh data points suggest that carbon deposition rates are slower for the more catalytically active material.

It was initially believed that no carbon would form with a mixture having a CO_2 to CH_4 weight ratio of 3.0. Five tubes were tested with this mixture at temperatures up to 2880°R. Complete blockage from carbon deposition occurred within 48 hr for all five tubes. Most severe carbon deposits occurred in regions of lowered T_w rather than at the maximum temperature locations. In the region of high T_w, small (order of 1 mil) coatings of pyrolytic carbon were noted. At cooler locations, both pyrolytic and amorphous carbon were found. A kinetically possible explanation[3] for the unexpected carbon deposits is that CO_2 reacts with the carbon surface to form an oxide surface structure. A unimolecular layer of CO is bonded to the carbon surface and thus activates the surface. A surface catalysis reaction occurs involving the chemisorption of methane on the activated carbon with the production of ethylene. Almost immediately, the ethylene decomposes

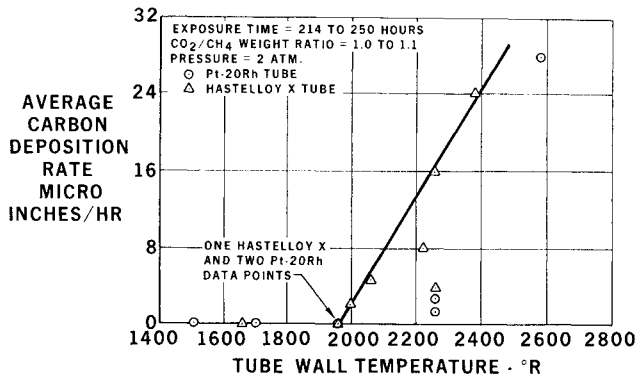

Fig. 2 Carbon deposition rate.

and deposits carbon at the surface site left free of oxygen by the evolution of water. The overall reaction equation for this is $(CO)^* + CH_4 \rightarrow H_2O + 2C + H_2$. The asterisk denotes the bonded carbon monoxide molecule which forms as follows: $CO_2 + C \rightarrow (CO)^* + CO$.

The water that forms offers a potential carbon stripping reaction, given by $H_2O + C \leftrightarrows CO + H_2$. One of the tubes examined had a pyrolytic carbon deposit thickness which increased rapidly in the direction of flow and then decreased. A longitudinal section of the tube revealed a venturilike channel remained. The carbon-stripping reaction may have caused this. The venturi effect has been observed by Clark[4] with pure methane, and he suggests another possible mechanism for this phenomenon.

Thruster Design

Two configurations of the 10-mlb thrust biowaste resistojet, Mark I and Mark II, have been fabricated. Mark I heater elements were fabricated in Pt-20Rh alloy. Nozzle geometry is identical to the life thruster and is nonoptimum for the biowaste propellants, having a nozzle exit-to-throat area ratio ϵ of only 32. Nozzle Reynolds numbers are higher with biopropellants than with hydrogen, suggesting that a higher ϵ be used.

Figure 3 shows exterior views of the Mark II thruster, which weighs 0.6 lb and has heater and nozzle parts made of Pt-20 Ir alloy. Design features are best described with reference to Fig. 1. The Mark II thruster has improved structural strength to withstand launch vibration and acceleration environments. Thermal energy distribution has been improved by increasing the pass 2 channel flow area and by tapering the wall thickness of the innermost heater element. A trumpet-shaped exit nozzle provides improved performance with the highly viscous nozzle flow, as well as increased structural rigidity between the inner heater element and outer case. Geometrically, $\epsilon \simeq 400$. The trumpet-shape effects a rapidly increasing divergence angle to an included angle of 70°. The effective area ratio is ~100. Nozzle throat entrance radius is relatively sharp per the recommendation of Rae.[5] Some radius is desired to minimize throat size changes due to erosion.

A thermal dam is used in gas pass 1 to minimize longitudinal heat conduction from the hot heater tubes. The dam consists

Table 2 Degree of reaction of an equimolar mixture of CO_2 and CH_4 at 2660°R and 2 atm

Elapsed time, msec	Mixture molecular weight	Mole fractions CH_4	Mole fractions CO_2	Mole fractions CO	Mole fractions H_2O	Mole fractions H_2	Solid carbon
1.0	29.56	0.4638	0.4845	0.0078	0.0078	0.0219	0.27×10^{-6}
4.1	28.87	0.4271	0.4649	0.0158	0.0158	0.0515	0.70×10^{-5}
10.0	28.39	0.4007	0.4518	0.0209	0.0209	0.0734	0.27×10^{-4}

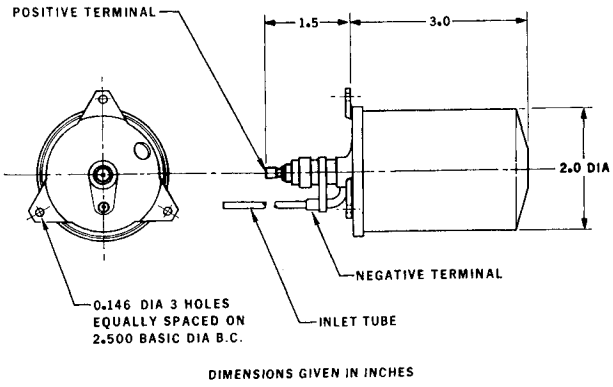

Fig. 3 10-mlb-Mark II resistojet.

of a thinner wall section for a short distance to increase thermal conduction resistance. Ohmic heating increases in the thinned section and is a tradeoff consideration in sizing the dam. The thermal dam results in reduced temperature at the expansion bellows permitting projection of the bellows further into the thruster heater cavity. This reduces overall length considerably and improves the strength of the thruster. Instrumentation is included in the Mark II design to measure the resistance of the innermost heater element. This will provide a power control signal and permit operation of the thruster closer to maximum design temperature.

Three Mark II thrusters have been fabricated. One will be subjected to vibration and acceleration loads after hot-firing to simulate an acceptance test prior to launch. The other two will be used to document thrusting performance on various biopropellants.

Thruster Performance

Figure 4 shows expected power requirements and specific impulses vs chamber gas temperature T_g entering an assumed optimum expansion nozzle, i. e., a nozzle with a geometry which maximizes the product of nozzle viscous expansion,

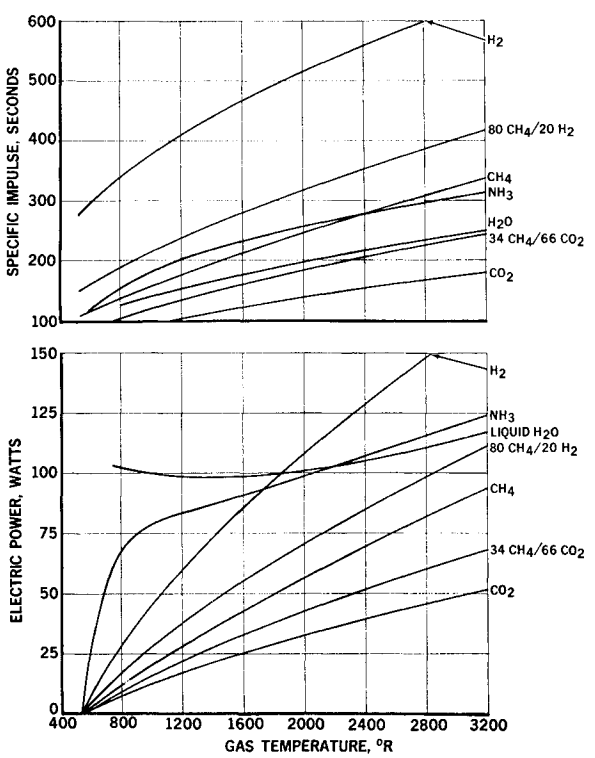

Fig. 4 Performance of 10-mlb resistojets-P_c = 2 atm.

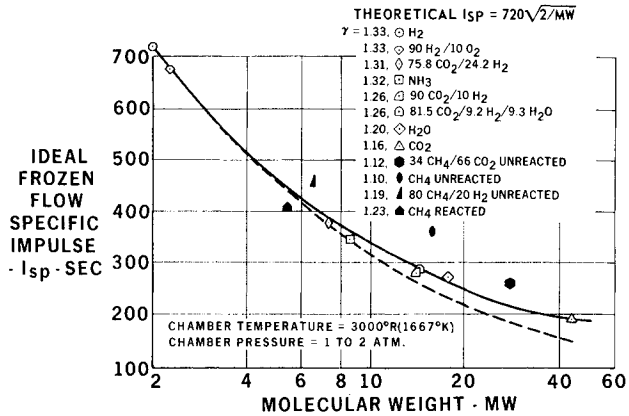

Fig. 5 Ideal frozen flow specific impulse correlation.

and divergence efficiencies for a specific T_g and propellant. The electric power requirements shown apply specifically to this resistojet heater concept, with appropriate heater efficiencies applied. For liquid propellants, a pre-evaporator is required; therefore, the power requirements shown for liquid water in Fig. 4 include losses for an electric pre-evaporator. A pre-evaporator suitable for operation in a zero-g environment is being developed for this resistojet. Thermal efficiencies in the high nineties have been demonstrated for a prototype evaporator. If steam is available, from a waste heat evaporator, for example, the electric power requirement is reduced significantly. For steam received at 735°R, for instance, the required-power curve would fall about $\frac{2}{3}$ of the way from the CO_2 to the $34CH_4/66CO_2$ curve.

Equilibrium chemistry is assumed for the Fig. 4 curves, except for methane-bearing propellants. Nonreacted chemistry is assumed and is appropriate for the CH_4, $80CH_4/20H_2$, and $34CH_4/66CO_2$ curves. For the biowaste resistojet temperatures, the degree of equilibrium decomposition of H_2, H_2O and CO_2 is not significant with mole fractions of the decomposition products less than 10^{-3}. The corresponding Fig. 4 curves are, therefore, realistic. The NH_3 curves are for equilibrium chemistry, which is not necessarily realistic. Ammonia does decompose at biowaste temperatures, but the degree of reaction is not certain. At the high temperature end the NH_3 curves are considered to be close to realistic.

The resistojets being developed are capable of achieving T_g's to 3000°R. A T_g of 2700°R is recommended, however, for long life. Thus, expected I_{sp} ranges from 160 sec for CO_2 to 570 sec for H_2. While methane offers better than 300 sec at full operating temperature, this performance cannot be practically utilized because of the carbon deposition problem. Assuming a threshold T_w of ~1960°R resulting in a T_g of 1800°R will apply to the propellants containing methane, then an I_{sp} of 230 sec appears possible with methane. If the resistojet is always to flow methane and T_w is limited to ~2000°R, materials other than noble metal alloys can be used. The present program is directed toward the development of a thruster for all biopropellant possibilities.

Figure 5 presents a simplified correlation of ideal-frozen flow-I_{sp} vs propellant molecular weight MW at T_g = 3000°R. Theoretically, $I_{sp} \propto (T_g/MW)^{1/2}$. This relationship follows from the limiting velocity corresponding to an infinite expansion to vacuum and the assumption of perfect gas. The specific heat ratio γ is considered constant in the derivation of this proportionality. In Fig. 5, those cases not containing methane correlate rather well as shown by a solid curve fit. Although γ is not constant for these cases (open symbols), γ decreases consistently with increasing MW. This is reflected by the systematic deviation away from a theoretical correlation shown as a dashed line referenced to the hydrogen point. Note that typical cases involving methane (solid symbols) do not correlate well with the open symbol cases. Reacted

Table 3 Mark I biowaste resistojet experimental performance summary

Propellant	F, g (mlb)	I_{sp}, sec	P_e, w	η^a
Air	4.39 (9.7)	158	53	0.54
H_2O^b	5.45 (12.0)	212	94.5	0.45
CO_2	6.48 (14.3)	133	87	0.43
CH_4^c	2.63 (5.8)	232	71	0.38
CH_4^d	4.46 (9.85)	185	63	0.51
72 CO_2 + 28 CH_4	5.10 (11.25)	176	94.5	0.42
67 CO_2 + 33 CH_4	5.07 (11.2)	182	94	0.43

[a] Over-all total power efficiency, $\eta \simeq (F \times Isp)/20.8\ (P_e + P_i)$ where F = thrust, g; I_{sp} = specific impulse, sec; P_e = electric power, w; and P_i = propellant power at inlet, w.
[b] Thruster supplied with steam at 775°R from pre-evaporator.
[c] Thrust slowly decreasing due to carbon deposition.
[d] Thrust constant at lower operating temperature.

methane falls low in I_{sp}; whereas the unreacted methane and methane mixtures fall high. This is the result of a particularly high specific heat relative to other gases on a molecular weight basis. For a given T_g, unreacted methane contains more available energy than other gases at the same MW and hence delivers a higher I_{sp}. The reacted methane point is low because of the large amount of dissociation energy lost in the assumed frozen nozzle flow.

Thrusting tests are in progress on the Mark II biowaste resistojet, but data are not yet available. The Mark I biowaste resistojet has been operated with several typical biowaste propellants. High-gas-temperature performance data are summarized in Table 3. The Mark I thruster has a nonoptimum nozzle and falls below expected optimum thruster performance. Over-all efficiencies listed in Table 3 are based on total input power. The overall total power efficiency is the useful axially-directed power leaving the thruster nozzle ratioed to the sum of the electric and propellant power put into the thruster.

Gas temperatures are not measured directly in the small 10-mlb resistojet. Rather, gas temperatures are estimated from energy balance and mass continuity calculations. In addition, an optical pyrometer reading is obtained for the outside of the heater at the strut connector end by viewing through the expansion bellows along the thruster axis. This surface temperature can be correlated to gas temperature. For the Table 3 data, T_g's are estimated to vary from 2400° to 2900°R. The 9.85-mlb CH_4 data point is an exception, with an estimated T_g of 1600° to 1900°R. The thruster was operated at the lower temperature to avoid carbon deposition.

Figure 6 compares Mark I resistojet data using the I_{sp} vs MW correlation. An arbitrary theoretical I_{sp} curve is indicated by a dashed line. The experimental data curve fits show the same deviation trend from the theoretical as for the ideal performance presented in Fig. 5. Note also, that the methane data point, corresponding essentially to unreacted flow, is relatively high, as predicted. This correlation technique offers the potential for determining whether methane is being decomposed or not. Recall from Fig. 5 that reacted methane performance falls below the theoretically expected performance when plotted at the corrected molecular weight. If a nonreacted molecular weight were assumed, the reacted point would fall on the theoretically expected curve still indicating clearly a reacted condition. To use this technique, it is necessary to operate a thruster at the same temperature

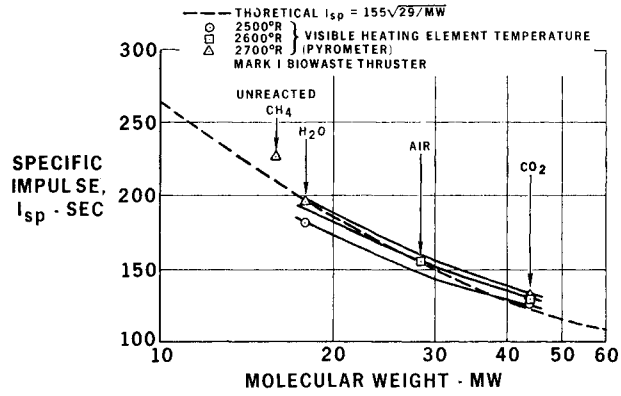

Fig. 6 Correlation of experimental specific impulse with propellant molecular weight.

with propellants having different molecular weights (e.g., H_2, H_2O, air, and CO_2) to establish baseline curves.

Conclusions

Resistojets with sufficiently high efficiency can satisfy attitude-control and drag-makeup propulsion requirements on manned space stations utilizing biowaste propellants. The 10-mlb-thrust, concentric-tubes thruster described herein can be scaled-up to match specific space-station requirements. The need for corrosion resistance at high structural temperature requirements in biowaste chemistry environments has directed attention to the noble metals for thruster heater parts. Presently, Pt-20Ir alloy is being used, because Pt-Rh alloy is susceptible to carbonyl corrosion in the presence of CO_2. The heater material also must have sufficient cold strength in the annealed condition to withstand launch vibration and acceleration loads, and adequate creep strength for thousands of hours of high-temperature operation.

The biowaste resistojet is expected to provide specific impulses ranging from 160 sec with CO_2 to 570 sec with H_2. These values correspond to heater element temperatures selected to provide a large temperature margin and assure long thruster lifetime.

References

[1] Greco, R. V., "Resistojet Control Systems for Advanced Manned Spacecraft," *Space/Aeronautics*, Vol. 51, No. 3, March 1969, pp. 82–88.

[2] Halbach, C. R., "Technology Development of a Biowaste Resistojet," First, Second and Third Quarterly Progress Reports, 25203, 25308 and 25310, Dec. 1969–June 1970, The Marquardt Co., Van Nuys, Calif.

[3] Yoshida, R. Y., Halbach, C. R., and Hill, C. S., "Life Test Summary and High Vacuum Tests of 10-mlb Resistojets," AIAA Paper 70-1136, Stanford, Calif., 1970.

[4] Clark, R. K., "Simulation of Pyrolysis-Gas Flow Through a Char Layer During Ablation," TN D-5464, Oct. 1969, NASA.

[5] Rae, W. J., "Final Report on a Study of Low-Density Nozzle Flows, with Application to Micro-Thrust Rockets," Al-2590-A-1, Dec. 1969, Cornell Aeronautical Lab., Buffalo, N.Y.